

Structural system identification including shear deformation of composite bridges from vertical deflections

Seyyedbehrad Emadi¹, Jose A. Lozano-Galant², Ye Xia^{*3}, Gonzalo Ramos¹ and Jose Turmo¹

¹ Department of Civil and Environmental Engineering, Universitat Politècnica de Catalunya (UPC) BarcelonaTECH, Barcelona, Spain

² Department of Civil Engineering, University of Castilla-La Mancha, Ciudad Real, Spain

³ Department of Bridge Engineering, Tongji University, Shanghai, China

(Received January 11, 2019, Revised August 25, 2019, Accepted September 8, 2019)

Abstract. Shear deformation effects are neglected in most structural system identification methods. This assumption might lead to important errors in some structures like built up steel or composite deep beams. Recently, the observability techniques were presented as one of the first methods for the inverse analysis of structures including the shear effects. In this way, the mechanical properties of the structures could be obtained from the nodal movements measured on static tests. One of the main controversial features of this procedure is the fact that the measurement set must include rotations. This characteristic might be especially problematic in those structures where rotations cannot be measured. To solve this problem and to increase its applicability, this paper proposes an update of the observability method to enable the structural identification including shear effects by measuring only vertical deflections. This modification is based on the introduction of a numerical optimization method. With this aim, the inverse analysis of several examples of growing complexity are presented to illustrate the validity and potential of the updated method.

Keywords: structural system identification; observability; shear deformation; vertical deflection; composite structures

1. Introduction

System Identification (SI) is a process of modeling an unknown system that has been employed in a number of engineering fields (Sirca Jr. and Adeli 2012, Altunişik *et al.* 2017). The discipline of SI aims to create mathematical models that characterize properly the system behavior. One of the pioneers in this approach was Friedrich Gauss who developed the Gauss-Newton method to find the values of parameters in a model of the trajectory to calculate the dwarf planet trajectories. SI began in the area of electronic engineering and, after a while, it has been extended to other fields of engineering (Gevers 2006, Pisano 1999). Structural system identification (SSI) is a part of the SI dealing with the construction of mathematical models to identify the structural parameters (such as flexural stiffnesses, axial stiffnesses or damping parameters) from the structural response (Pajonk 2009).

A number of methods are proposed for SSI in the literature (Liao 2012, Lozano-Galant 2013, Yan and Golinval 2005). These methods can be classified according to the excitation test type as dynamic (Breuer *et al.* 2015, Dowling *et al.* 2012, Li *et al.* 2017a, Górski *et al.* 2018) or static (Thirumalaiselvi *et al.* 2016, Walsh and González 2009, Lee *et al.* 2010). SSI methods might be also classified as a parametric (Lozano-Galant *et al.* 2013, Gracia-Palencia *et al.* 2015) or non-parametric methods (Karabelivo *et al.* 2015, Mei *et al.* 2016). Parametric methods rely on the

physical based models, while in non-parametric ones, parameters do not have any physical meaning. In non-parametric methods, parameters are identified directly with optimization procedures that minimize the difference between the predicted structural response and the measured ones. For parametric SSI methods, a mathematical representation of the structural behavior is required. The most common way to do this modeling is based on the Stiffness Matrix Method (SMM) (Hou *et al.* 2015, Khayat *et al.* 2017a, b, Li *et al.* 2014, 2017b, Araki and Miyagi 2005). The details of the main SSI methods proposed in the literature are presented in (American Society of Civil Engineers 2013).

Despite the importance of shear deformation in some structures, it is overlooked by most of SSI methods. For most structures, deflection due to the shear is much smaller than the deflection due to the bending, thus this phenomenon can be ignored. In these cases, shear effects are considered as modeling errors in the mathematical models (such as any property in the model assumed with a wrong value). Nevertheless, in some structures (such as deep beams, shear walls, short span beams, or thin-web bridges) shear effects might play an important role. In this case, they should not be neglected and should be introduced into the formulation.

Most traditional SSI methods are not able to observe correctly the parameters of a structure (such as bending stiffness) when shear deformation is not negligible. SSI methods based on SMM normally use elementary beam theory, underestimating deflections and overestimating the natural frequencies since the shear deformation effect is disregarded (Sayyad 2011). Timoshenko (1921) was the

*Corresponding author, P.E., Associate Professor,
E-mail: yxia@tongji.edu.cn

first one who included shear effects into the beam theory. This approach is known as Timoshenko beam theory. Due to the complexity of this theory, SSI models are mostly based on Euler–Bernoulli beam theory which only includes axial and flexural deformation and shear effects are neglected in the analysis. Some authors studied the effect of shear deformation in their SMM models of composite structures (Kumar and Srinivas 2018, Nguyen and Tran 2018, Singh and Chakrabarti 2017). Moreover, Soto and Rojas (2017) proposed a new SMM's formulation including shear effects for the modeling fixed–end moments of I-sections. The effects of shear deformations in recursive matrix method for sandwich plate were also studied by (Huo *et al.* 2017). The impact of shear effects in steel-concrete composite structures is studied by (Yang *et al.* 2018) and (Wang *et al.* 2018). Tomas *et al.* (2018) included the effects of shear deformations in Observability Method (OM). This method introduced the shear formulation into the SMM. Among the advantages of the method, it is to highlight the fact that it provided for the first time in the literature parametric equations of the shear estimates by the OM. The main inconvenience of this methods is that the measurement set requires both rotations and vertical deflections to identify mechanical properties. OM is a parametric SSI method based on the system of equations of the SMM. In this procedure, the axial and flexural stiffnesses are obtained from the static deformations measured in a static test. OM has proved its efficiency in different structural typologies (such as trusses, beams, frame structures and cable-stayed bridges) (Lozano-Galant *et al.* 2014, 2015, Nogal *et al.* 2015, Castillo *et al.* 2007, 2016, Lei *et al.* 2016, 2017a, 2019).

According to the literature, the only detailed study which addressed the particular effects of this deformation in the observability method (OM) is Tomas *et al.* (2018). However, this failed to observe parameters just using vertical deflections measured from controlled static tests due to the complexity of equations. OM always required measurement sets that combined rotations and deflections to take into account shear deformations. However, many infrastructure control only relies on deflection measurement (e.g., surveying through topography), being rotation measurement and the use of clinometers much more scarce (Abdo 2012). So it might be practical to have a method that only requires vertical deflections. Also, information which can be produced by measuring vertical displacement are more reliable than rotation and international standards deal with vertical deformation (Vicente *et al.* 2018, AASTHO 2017, European Committee for Standardization 2005).

The aim of this paper is (1) to present a parametric numerical method for static structural identification when shear behavior is taken into account using measurement sets containing only deflections (avoiding the need for including rotations in the measurement sets from previous methods); (2) to evaluate the robustness of the method; (3) to present a potential practical application of the method.

This article is organized as follows: In Section 2, the SSI including shear deformations with OM is briefly presented. A simply supported beam is analyzed to illustrate the inability of the method presented in (Tomas *et al.* 2018) to

identify mechanical properties by measuring just vertical deflections. Section 3 introduces constrained observability method (COM) (Lei *et al.* 2017b) COM to enable the structural identification by measuring only vertical deflections. To illustrate the application of this algorithm, a step by step example of a simply supported beam is presented. In addition, another numerical example of an intermediate construction stage of a cantilever bridge is analyzed. Finally, the summary is drawn in Section 4.

2. Observability method including shear effects

From 2D beam element direct SMM of a structure loaded in its plane, the nodal equilibrium equations might be written as

$$[K] \cdot \{\delta\} = \{f\} \quad (1)$$

where the displacements vector $\{\delta\}$ contains the horizontal, vertical, and rotational displacements, the external force vector $\{f\}$ contains the horizontal forces, vertical forces, and moments and the global stiffness matrix $[K]$ contains the stiffness of the beam elements. The stiffness matrix $[K]$ contains the information of flexural stiffness EI , axial stiffness EA and length L , where E , I and A are Young modulus, inertia and area, respectively. According to the literature, in 1968, Przemieniecki added shear deformation to the stiffness matrix for the very first time. Unlike traditional stiffness matrix, a coefficient \emptyset known as the shear parameter appears in some elements of Przemieniecki's stiffness matrix. This parameter is as follows

$$\emptyset = \frac{12EI}{GA_v L^2} \quad (2)$$

where A_v is the shear area and G is the shear modulus. Also, the coefficient ν is Poisson's ratio as it shows in Eq. (3). Analysis of Przemieniecki's stiffness matrix shows that shear parameter \emptyset appears in the denominator of most terms. In order to solve this problem, Tomas *et al.* proposed the following change of variable implying a shear parameter Q . This OM shear parameter is described as follows (Eq. (4))

$$G = \frac{E}{2(1 + \nu)} \quad (3)$$

$$Q = \frac{\emptyset}{1 + \emptyset} \quad (4)$$

After replacing the shear parameter \emptyset by OM shear parameter Q , the stiffness matrix presented can be updated as

$$[K] = \begin{bmatrix} \frac{EA}{L} & 0 & 0 & -\frac{EA}{L} & 0 & 0 \\ 0 & \frac{12EI}{L^3} - \frac{12EIQ}{L^3} & \frac{6EI}{L^2} - \frac{6EIQ}{L^2} & 0 & -\frac{12EI}{L^3} + \frac{12EIQ}{L^3} & \frac{6EI}{L^2} - \frac{6EIQ}{L^2} \\ 0 & \frac{6EI}{L^2} - \frac{6EIQ}{L^2} & \frac{4EI}{L} - \frac{3EIQ}{L} & 0 & -\frac{6EI}{L^2} + \frac{6EIQ}{L^2} & \frac{2EI}{L} - \frac{3EIQ}{L} \\ -\frac{EA}{L} & 0 & 0 & \frac{EA}{L} & 0 & 0 \\ 0 & -\frac{12EI}{L^3} + \frac{12EIQ}{L^3} & -\frac{6EI}{L^2} + \frac{6EIQ}{L^2} & 0 & \frac{12EI}{L^3} - \frac{12EIQ}{L^3} & -\frac{6EI}{L^2} + \frac{6EIQ}{L^2} \\ 0 & \frac{6EI}{L^2} - \frac{6EIQ}{L^2} & \frac{2EI}{L} - \frac{3EIQ}{L} & 0 & -\frac{6EI}{L^2} + \frac{6EIQ}{L^2} & \frac{4EI}{L} - \frac{3EIQ}{L} \end{bmatrix} \quad (5)$$

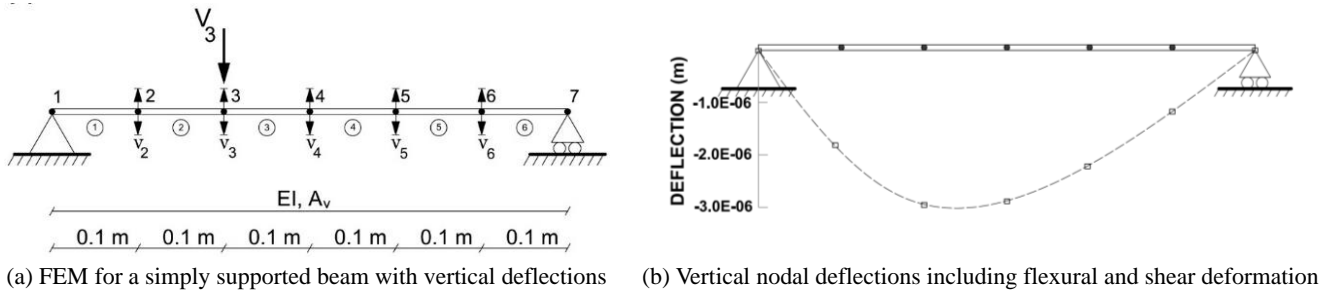


Fig. 1 Example 1

Once the geometry, the boundary conditions and the applied nodal forces in a certain static load test are defined, some displacements can be measured to identify the unknown mechanical properties in the SMM. To do so, an inverse analysis is performed. The known information is clustered in a subset δ_1 and f_1 of $\{\delta\}$ and $\{f\}$, respectively and the subset δ_0 of $\{\delta\}$ and a subset f_0 of $\{f\}$ are assumed as unknown information. The Eq. (1) can be rewritten as follows

$$[K^*] \cdot \{\delta^*\} = \begin{bmatrix} K_{00}^* & K_{01}^* \\ K_{10}^* & K_{11}^* \end{bmatrix} \cdot \begin{Bmatrix} \delta_0^* \\ \delta_1^* \end{Bmatrix} = \begin{Bmatrix} f_0 \\ f_1 \end{Bmatrix} = \{f\}, \quad (6)$$

In order to join the unknown variable in the left-hand side and the known variable in the right-hand side, the Eq. (6) is rearranged as

$$[B] \cdot \{z\} = \begin{bmatrix} K_{10}^* & 0 \\ K_{00}^* & -I \end{bmatrix} \cdot \begin{Bmatrix} \delta_0^* \\ f_0 \end{Bmatrix} = \begin{Bmatrix} f_1 - K_{11}^* \delta_1^* \\ -K_{01}^* \delta_1^* \end{Bmatrix} = \{D\}, \quad (7)$$

where 0 and I are the null and the identity matrices, respectively. To evaluate if the system has a solution, the null space $[V]$ of matrix $[B]$ should be calculated and check that $[V]^T \{D\} = 0$. If the equation holds, the system is compatible; otherwise, it has no solution. The general solution (the set of all solutions) of the system (7) has the structure (Castillo *et al.* 2000, 2002)

$$\{Z\} = \{Z_p\} + [V] \cdot \{\rho\}, \quad (8)$$

where $\{Z_p\}$ is a particular solution of the system (8). $[V] \cdot \{\rho\}$ is the set of all solutions of the associated homogeneous system of equations (a linear space of solutions, where the columns of $[V]$ are a basis of this linear space and the elements of the vector $\{\rho\}$ are arbitrary real values that describe the coefficients of all possible linear combinations). It should be noted that a variable has a unique solution not only when matrix $[V]$ has zero dimension (it does not exist), but when the associated row in matrix $[V]$ is null. Thus, the examination of matrix $[V]$ and identification of its null rows leads to the identification of the subset of variables with a unique solution in vector $\{Z\}$. It is interesting to note that if all parameters of vector $\{Z\}$ are not observed from the null space, any deflection, force or parameter observed after the initial OM analysis will be used to observe new parameters by using a recursive process. For more information about

this process, the reader is addressed to (Lozano-Galant *et al.* 2013, Timoshenko 1921).

According to the literature, more reliable information can be produced from measuring vertical displacement than rotation and most of international standards deal with vertical deformation (Vicente *et al.* 2018, AASTHO 2017, European Committee for Standardization 2005). So it is useful to provide a method that allows SSI from measured vertical deflections. Traditional OM including shear deformation presented in (Tomas *et al.* 2018) fails identifying shear parameters with measurement sets including only vertical deflections. In fact, the measurement of rotations is required to observe any parameter by OM. To show the inability of OM to identify material properties with only measured vertical deflection an illustrative example is analyzed in the following section.

2.1 Example 1: Simply supported beam with vertical deflections

Consider the 0.6 m long simply supported beam modelled with 7 nodes and 6 Timoshenko beam elements in Fig. 1(a), where, v_j , with j (1 to 7) represents the vertical deflection for each node. Beam has a constant cross section and the value of Young modulus, Poisson's ratio, shear area, cross sectional area and inertia of all elements along the beam are constant. Properties of this simply supported beam are listed on Table 1. The boundary conditions of the structure are horizontal and vertical displacements restricted in node 1 and vertical displacement restricted in node 7 (this is to say, $u_1 = v_1 = v_7 = 0$) and the only external force applied in this numerical loading test is a concentrated vertical force in node 3 of 100 kN ($V_3 = 100$ kN). The vertical deflections obtained from the software Midas/Civil of this structure are presented in Fig. 1(b). Measurement errors in this paper are neglected.

For this inverse analysis of the structure, V_3 , the length of the elements, Poisson's ratio and Young modulus are assumed as known, while the inertia I and the shear area A_v are assumed as unknown. Since no horizontal force is applied in this example, the axial resistant mechanisms are not activated. So the terms associated with axial behavior are removed from general SMM system of equations. Since the only two unknown parameters assumed in example 1 are A_v and I , the measurement of at least two deformations is required to identify their values. Nevertheless, no set of vertical deflections enables the proper identification of the unknown parameters.

the unknowns. Any number can be used as initial value, but in order to ease the convergence in the optimization process, a ratio with the theoretical values (e.g., between 0.5 to 1.5) is advised.

In the COM (Lei *et al.* 2017b), variables are classified in one of the following three categories: (1) Coupled variables V_c (Iw_j and Qw_j from example 1); (2) Single variables v_{s1} (I and Q from example 1), which already exist in the unknown $\{Z\}$ vector; (3) Single variables V_{s2} (w_j from example 1), which did not exist in the unknown vector $\{Z\}$ from OM. The new vector $\{Z\}$ is named $\{Z^*\}$ and it is a combination of vector $\{Z\}$ and the new single variables V_{s2} . In order to create an objective function for a numerical optimization process and take into the account the new unknowns V_{s2} , Eq. (7) can be rewritten as

$$\{\epsilon\} = [B^*] \cdot \{Z^*\} - \{D\}, \quad (10)$$

where ϵ is the residuals of the equations which is a vector with the same number of rows of the original matrix B and $B^* = [B^{N_{eq} \times N_z} | \Omega^{N_{eq} \times N_{s2}}]$ is obtained by adding a null matrix Ω to the matrix B calculated from the last recursive step of SSI by OM. The size of this null matrix Ω is $N_{eq} \times N_{s2}$. N_{eq} and N_z , explain the number of equations and the number of unknowns in $\{Z\}$, respectively. N_{s2} explains the number of new single unknowns in V_{s2} .

The objective function of the minimization problem is determined by minimizing the square sum of the residuals in Eq. (10). In order to reach a certain level of efficiency in the COM optimization process, variables of Eq. (10) should be normalized. The optimization toolbox of Matlab (MATLAB and Optimization Toolbox Release 2017) has been used to obtain the optimal solution of the objective function. In order to limit the computational expense and the time of the optimization process, the stopping criterion has been defined based on the value of the norm of the residual vector, ϵ (Eq. (10)). When this is smaller than $1e^{-8}$ the iterations stop. The algorithm for SSI by COM is summarized as follows:

Step 1: Apply SSI by OM to check whether any unknown is observed. If so, update the input and reinitiate OM until no new unknowns are observable. If full observability is achieved, there is no need to go to the COM process, otherwise go to the step 2.

Step 2: Obtain the Eq. (7) from the last step of OM recursive process then generate the new unknown vector of Z^* included Coupled variables V_c ; as well as single variables V_{s1} and V_{s2} .

Step 3: Add a null matrix $[\Omega]$ to the matrix $[B]$ to generate $[B^*]$, in order to contain V_{s2} in Z^* without violating system.

Step 4: Obtain the normalized unknown parameters.

Step 5: Guess the initial values of unknowns parameters of Z^* vector, set the bound for the solution and solve the optimization process to find the minimized value for the residual vector, ϵ .

A summary of the procedure is shown in the flow chart in Fig. 2. For more information about the COM, reader is addressed to (Lei *et al.* 2017b).

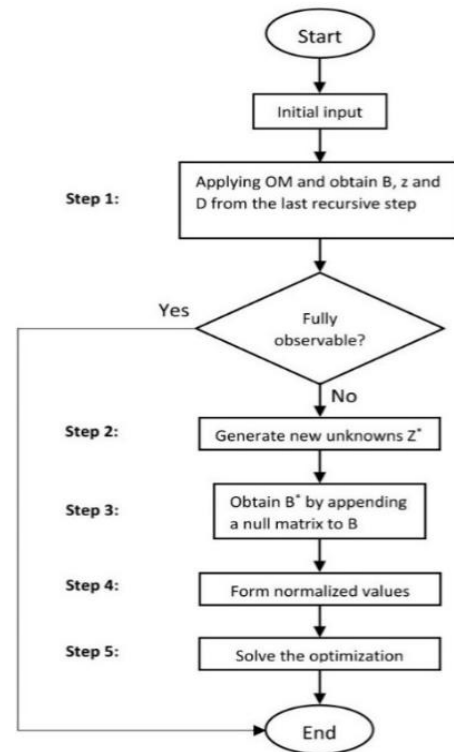


Fig. 2 Flow chart of structural system identification by COM

The majority of SSI methods is based on the Euler-Bernoulli beam theory. Originally, COM method is not able to consider the effect of shear in measurements. To include this phenomenon, in this work, equations are updated to the procedure proposed by Tomás *et al.* (2018). With this new updated method, the problem of linearization in OM variables is solved and equations related to shear stiffnesses are taken into account. In order to illustrate the applicability of the method the same structure from Example 1 is analyzed below.

3.1 Example 1 revisited: simply supported beam with vertical deflections (COM)

The beam of example 1 is recalculated by the COM with the same parameters. The unknown inertia and shear parameter can be obtained not only with all possible vertical deflections (5 degrees of freedom) but also just with 2 deflections (e.g., v_2 and v_3). The $\{Z\}$ vector of example 1 with just measuring v_2 and v_3 is presented in Eq. (11), but in order to apply COM, $\{Z^*\}$ should be calculated. The vector $\{Z^*\}$ of example 1 with a measured vertical deflection in nodes number 2 and 3 is presented in Eq. (12). As highlighted in the previous section, in the COM, terms of $\{Z^*\}$ vector should satisfy certain nonlinear constrains, e.g., $\{Q_1 w_1 = Q_1 \cdot w_1\}$, these constraints are neglected in OM due to the linearity of equations which lead to a failure of the identification of the mechanical properties.

Numerical information from Table 1 is multiplied by different random coefficients ranging from 0.5 to 1.5 to generate initial values for COM process. According to the results, the optimization converges to the exact values of

inertia and OM shear parameter after few iterations. In the following comparison, the evolution of shear area and inertia ratio throughout the iterative process for different initial values (0.5 for shear area and 1.5 for inertia) are presented in Figs. 3(a)-(b), respectively.

$$Z = \begin{bmatrix} I \\ Iv_4 \\ Iv_5 \\ Iv_6 \\ Iw_1 \\ \cdot \\ \cdot \\ Iw_7 \\ Q \\ Qv_4 \\ Qv_5 \\ Qv_6 \\ Qw_1 \\ \cdot \\ \cdot \\ Qw_7 \\ H_1 \\ V_1 \\ V_7 \end{bmatrix}, \tag{11}$$

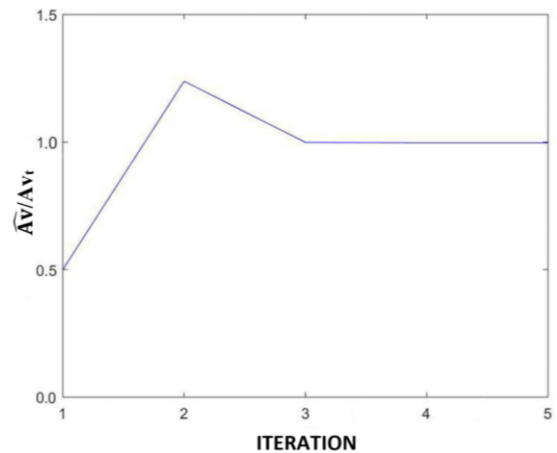
$$Z^* = \begin{bmatrix} I \\ I.v_4 \\ I.v_5 \\ I.v_6 \\ I.w_1 \\ \cdot \\ \cdot \\ I.w_7 \\ Q \\ Q.v_4 \\ Q.v_5 \\ Q.v_6 \\ Q.w_1 \\ \cdot \\ \cdot \\ Q.w_7 \\ H_1 \\ V_1 \\ V_7 \end{bmatrix} \tag{12}$$

This example far from proving the strength of COM, in the following section a more complex example is presented to illustrate the potential of the developed tool.

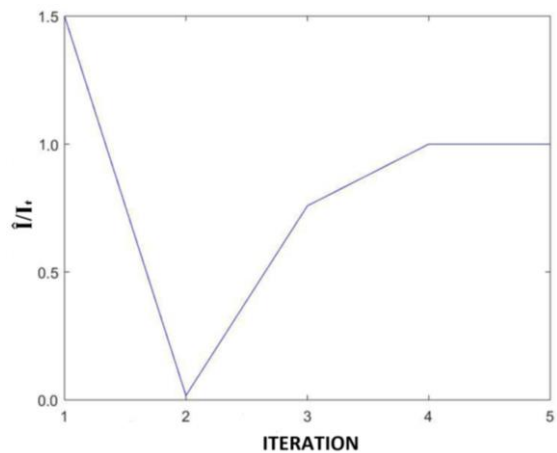
3.2 Application to a composite bridge

To illustrate the possible application of the COM to an actual structure, the problem of the construction of a bridge by the balanced cantilever method is presented here. In such

a construction method, deflections have to be anticipated in advance to calculate the precamber with which the different segments of the structure have to be built. In order to update this precamber for every step during construction, a thorough topographic surveying is usually performed. This information can be used for model updating via an inverse analysis. Even though shear deflections might not play a very important role for a full developed cantilever, modelling error of not taking into account shear effects for the first segments, might lead to an inaccurate estimation of the bending stiffness. To illustrate this and the possible application of this method, a simplified model of the Yunbao Bridge over the Yellow River in China (see Fig. 4) is studied in this section. The structure span is 90m long. An intermediate construction stage is considered in this example. This model includes the construction of two symmetric cantilevers. The length of the standard deck segments is 4.5 m and the length of the segment over the pile, 2.5 m. The total length of the studied construction stage is 29.5 m. The mechanical and material properties



(a) Evolution of shear area parameter ratio throughout the iterative process. Where $(A_v)^{\hat{}}$ is the estimated value of shear area and A_{vt} is the exact value of shear area



(b) Evolution of inertia ratio throughout the iterative process. Where $I^{\hat{}}$ is the estimated value of inertia and I_t is the exact value of inertia

Fig. 3 Evaluation of shear area and inertia ratio throughout the iterative process



Fig. 4 Composite bridge on site (China) (Dong *et al.* 2017)

Table 2 Properties of the Finite Element Model of the Bridge

Area [m ²]	12.52
Shear area [m ²]	9.83
Inertia [m ⁴]	35.62
Steel young's modulus [GPa]	210
Concrete young's modulus [GPa]	35

defined by the method of the transformed section (Chen and Yen 1980) are listed in Table 2.

Actual site data is not considered in this structure and the structural response is simulated numerically. Effects of creep and shrinkage in concrete are overlooked. The load test used simulates the movement of the formwork traveler (Fig. 5).

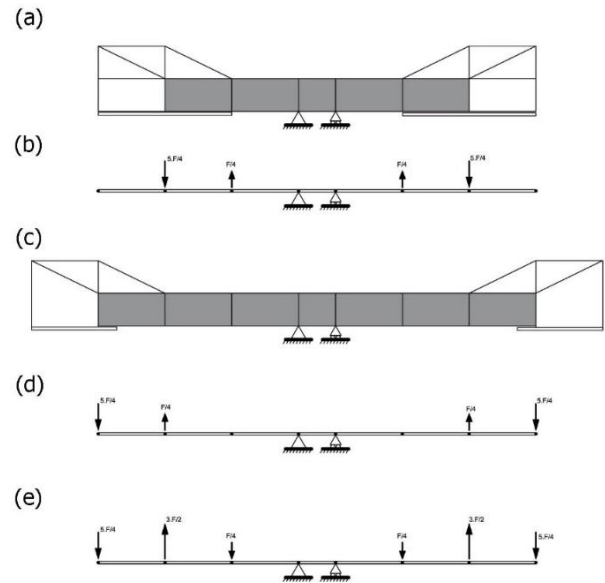


Fig. 5 Definition of the load case: (a, b) Stage i. (c, d) Stage i+1. (e) Load case used for the inverse analysis

The weight F of the formwork traveler (weight of formwork included is considered as the 60 % of the weight of the segment (1041 kN). The effect of each form traveler in the deck is considered as two vertical forces. The values of these two forces are $0.25F$ and $1.25F$ (226 kN, upwards and 1267 kN, downwards). Load case of the bridge model is calculated by reducing the effects of the stage i (Fig. 5(a)), from stage $i+1$ (Fig. 5(c)), wherein the formwork traveler is moved forward to the next segment. Load cases of the

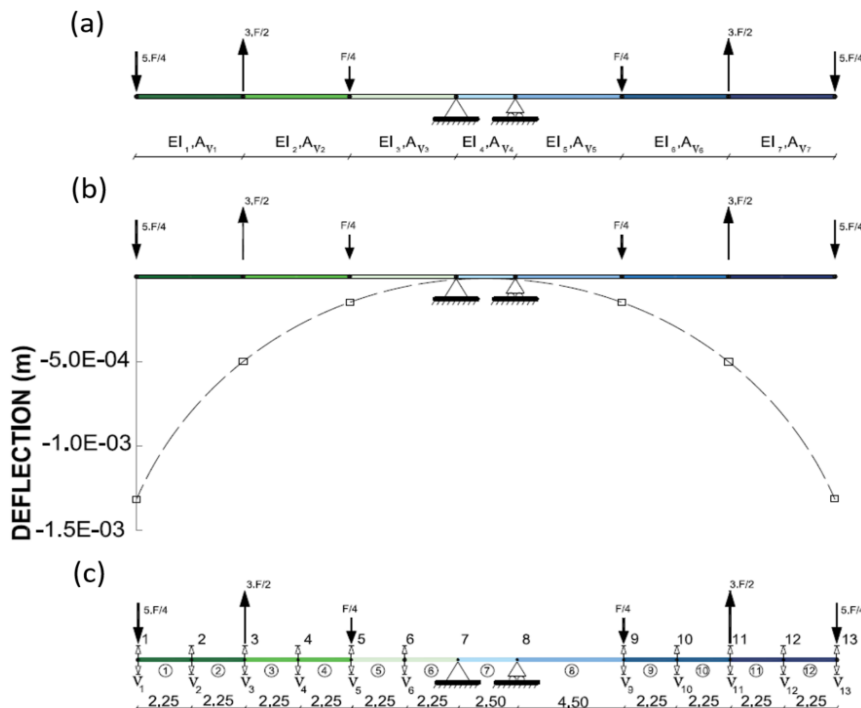


Fig. 6 Example 2. (a) FEM of the bridge with load case used for inverse analysis; (b) Variation of vertical deflections in this loading case with shear deformation; (c) New FEM with 13 nodes and 12 elements used for inverse analysis (dimensions in m)

stages i and $i+1$ are expressed in Figs. 5(b) and (d), respectively. The consequent load case introduced in the simulation is shown in Fig. 5(e). It is to highlight that the vertical resultant of such forces in each side of the cantilever is zero.

This structure is simulated by the simplified FEM presented in Fig. 6(a). This FEM includes 7 elements and 6 point loads. Software Midas/Civil is used in order to calculate the vertical deflections in the nodes of the structure presented in Fig. 6(b). For brevity, in the inverse analysis, Young modulus of all elements are considered as known parameters. Due to the fact that axial stiffness is not activated in this example, only flexural behavior is analyzed. For this reason, the terms related to the axial behavior are removed from equations (as axial stiffness are not activated with vertical forces). Because of loading case, shear area in elements number 3, 4 and 5 are not activated, so shear area in these elements cannot be observed in the inverse analysis. The shear area and inertia of all other

Table 3 Initial value coefficient of the Bridge Unknown Properties

I1	0.791
I2	0.688
I3	1.078
I4	1.486
I5	0.963
I6	0.941
I7	1.230
Q1	1.312
Q2	1.255
Q6	0.944
Q7	0.618

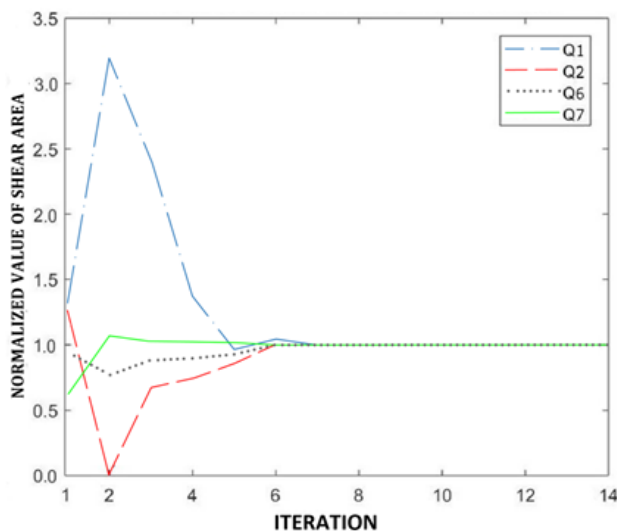
beam elements (that is to say $I_1, I_2, I_3, I_4, I_5, I_6, I_7$ and $A_{v1}, A_{v2}, A_{v6}, A_{v7}$) are assumed as unknowns.

In order to identify the 11 unknown mechanical properties at least, 11 measurements are required. As it was showed before, OM is not able to identify mechanical properties only with vertical deflections. However, it is examined and it is confirmed that no results were obtained with the measurement set of all possible vertical deflections (it is to say $v_1, v_2, v_3, v_4, v_5, v_6, v_9, v_{10}, v_{11}, v_{12}, v_{13}, v_{14}, v_{15}, v_{16}$) proposed for FEM presented in Fig. 6(c) when traditional OM is applied. To observe parameters with OM, the variation of deflection and rotation should be taken into account. In order to observe parameters just by vertical deflection in bridge example, COM is applied. Table 3 presents the initial value coefficient of different unknown inertia and shear area which is randomly chosen between 0.5 and 1.5 for the optimization process.

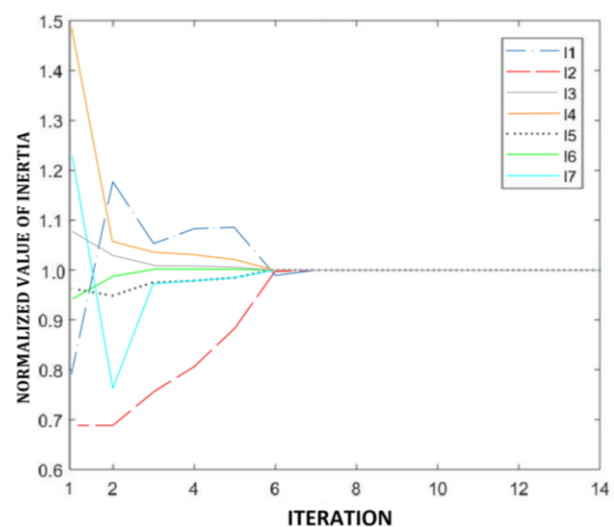
COM, managed to observe unknown shear area and inertia in 14 iterations, the evolution of shear area and inertia ratio throughout the iterative process, are presented in Figs. 7(a)-(b), respectively.

To prove the consistency of the new method, 200 analyses with random initial value coefficients between 0.5 and 1.5 are conducted for the bridge. From 200 analyses, in 62 analyses the optimization process was not convergent to the solution and no result was acquired, 37 results of optimization process were removed, due to the fact that the result did not have any physical sense (nonsense values e.g., negative values). The normalized average, standard deviation and coefficient of variation of the remaining results as well as the mode is presented in Table 4.

Tomas *et al.* (2018) compared differences between the estimated flexural stiffnesses (\hat{EI}) and the actual values (EI) in the seven elements of the bridge example without including the shear effects into the stiffness matrix of OM. According to this work when shear deformations are included into the measurements (error free measurements), significant errors (e.g., -65,5 % in segments 1 and 7 or



(a) Evolution of shear area parameters ratio throughout the iterative process



(b) Evolution of inertia ratio throughout the iterative process

Fig. 7 Evolution of shear area and inertia ratio throughout the iterative process

Table 4 Obtained results from random initial values

	Average	CoV	Standard deviation
I1	1.000	0.001	0.000
I2	1.000	0.002	0.001
I3	0.975	2.279	0.791
I4	0.993	12.229	4.324
I5	0.969	2.888	0.996
I6	0.999	0.004	0.002
I7	1.000	0.001	0.001

+26,7% in segments 2 and 6) appear in the observed flexural stiffnesses in OM. As it can be seen for table 4, these differences are greatly reduced with COM.

However, the shear area of some elements is not activated due to the loading case, making impossible the observation of shear areas of elements 5, 6, 7 and 8. This example proves the efficiency of the proposed COM to estimate inertia when shear effects are taken into account.

4. Conclusions

Most Structural System Identification (SSI) methods neglect shear deformation as this phenomenon is usually negligible in comparison with flexural deformation. However, it can play a significant role in some structures, as deep beams. According to the literature, the only detailed study which addressed the particular effects of this deformation in static SSI tests is the observability method (OM). However, this failed to observe parameters just using vertical deflections measured from controlled static tests due to the complexity of equations. OM always required measurement sets that combined rotations and deflections to take into account shear deformations. However, many infrastructure control usually relies on deflection measurement (e.g., surveying through topography), being rotation measurement and the use of clinometers much more scarce. So it might be practical to have a method that only requires vertical deflections. To fill this gap, this paper introduces the effects of shear deflections on the constrained observability method (COM). This method adds some nonlinear constraints to OM and, hence, the complex system of analytical equations is solved numerically after including the nonlinear constraints.

In the paper, a simply supported beam is studied in order to show the inability of OM to observe any parameter just by vertical deflections when shear effects are considered. To solve this problem, the formulation of constrained observability method (COM) is updated to include shear deformation. The COM performance in a simply supported beam shows the power of the new method to observe the value of the structural parameters just by vertical deflections. To show the applicability of the COM on a thin web structure, a simplified model of an intermediate construction stage of a cantilever composite bridge in China is studied. The results of this study show how the value of material properties can be observed by COM when the

shear effects are taken into account in the equations and the measurement sets only include vertical deflections. The robustness of the numerical method is also evaluated.

This research presents the application of the method for error free measurements sets. Possible modelling errors have been also neglected. The effect of the measurement errors and the modelling errors will be studied in the future. Application to the method to the actual measuring sets from real structures is also envisaged.

Acknowledgments

The authors are indebted to the Spanish Ministry of Economy and Competitiveness for the funding provided through the research project BIA2013-47290-R, BIA2017-86811-C2-1-R directed by José Turmo and BIA2017-86811-C2-2-R. All these projects are funded with FEDER funds. The support to the corresponding author from National Natural Science Foundation of China (51978508) is also acknowledged.

References

- AASSTHO (2017), LRFD Bridge Design Specifications, (8th Edition), American Association of State Highway and Transportation Officials; Washington, DC, USA.
- Abdo, M. (2012), "Parametric study of using only static response in structural damage detection", *Eng. Struct.*, **34**, 124-131. <https://doi.org/10.1016/j.engstruct.2011.09.027>
- Altunisik, A.C., Gunaydin, M., Sevim, B. and Adanur, S. (2017), "System identification of arch dam model strengthened with CFRP composite materials", *Steel Compos. Struct., Int. J.*, **25**(2), 231-244. <https://doi.org/10.12989/scs.2017.25.2.231>
- Araki, Y. and Miyagi, Y. (2005), "Mixed integer nonlinear least-squares problem for damage detection in truss structures", *J. Eng. Mech.*, **131**(7), 659-667. [https://doi.org/10.1061/\(ASCE\)0733-9399\(2005\)131:7\(659\)](https://doi.org/10.1061/(ASCE)0733-9399(2005)131:7(659))
- American Society of Civil Engineers (2013), Structural Identification of Constructed Systems, American Society of Civil Engineers, Reston, VA, USA.
- Breuer, P., Chmielewski, T., Górski, P., Konopka, E. and Tarczyński, L. (2015), "Monitoring horizontal displacements in a vertical profile of a tall industrial chimney using Global Positioning System technology for detecting dynamic characteristics", *Struct. Control Health Monitor.*, **22**(7), 1002-1023. <https://doi.org/10.1002/stc.1730>
- Castillo, E., Cobo, A., Jubete, F., Pruneda, R.E. and Castillo, C. (2000), "An orthogonally based pivoting transformation of matrices and some applications", *SIAM J. Matrix Anal. Appl.*, **22**(3), 666-681. <https://doi.org/10.1137/S0895479898349720>
- Castillo, E., Jubete, F., Pruneda, R.E. and Solares, C. (2002), "Obtaining simultaneous solutions of linear subsystems of equations and inequalities", *Linear Algebra Appl.*, **364**(1-3), 131-154. [https://doi.org/10.1016/S0024-3795\(01\)00500-6](https://doi.org/10.1016/S0024-3795(01)00500-6)
- Castillo, E., Conejo, A.J., Pruneda, R.E. and Solares, C. (2007), "Observability in linear systems of equations and inequalities: applications", *Comput. Operat. Res.*, **34**(6) 1708-1720. <https://doi.org/10.1016/j.cor.2005.05.035>
- Castillo, E., Nogal, M., Lozano-Galant, J.A. and Turmo, J. (2016), "Solving some special cases of monomial ratio equations appearing frequently in physical and engineering problems", *Math. Problems Eng.* <http://dx.doi.org/10.1155/2016/9764913>

- Chen, Y.S. and Yen, B.T. (1980), "Analysis of Composite Box Girders", Report N0 380.12; Fritz Engineering Laboratory Library.
- Deretić-Stojanović, B. and Kostic, S.M. (2017), "A simplified matrix stiffness method for analysis of composite and prestressed beams", *Steel Compos. Struct., Int. J.*, **24**(1), 53-63. <https://doi.org/10.12989/scs.2017.24.1.053>
- Dong, X. Zhao, L. Xu, Z. Du, S. Wang, S. Wang, X. and Jin, W. (2017), "Construction of the Yunbao Bridge over the yellow river", EASEC-15; Xi'an, China.
- Dowling, J., O'Brien, E.J. and González, A. (2012), "Adaptation of Cross Entropy optimization to a dynamic Bridge WIM calibration problem", *Eng. Struct.*, **44**, 13-22. <https://doi.org/10.1016/j.engstruct.2012.05.047>
- Eurocode (2005), Design of Concrete Structures—Concrete Bridges—Design and Detailing Rules, European Committee for Standardization: Brussels, Belgium.
- Gevers, M. (2006), "A personal view of the development of system identification: A 30-year journey through an exciting field", *IEEE Control Syst.*, **26**(6), 93-105. <https://doi.org/10.1109/MCS.2006.252834>
- Górski, P., Stankiewicz, B. and Tataru, M. (2018), "Structural evaluation of all-GFRP cable-stayed footbridge after 20 years of service life", *Steel Compos. Struct., Int. J.*, **29**(4), 527-543. <https://doi.org/10.12989/scs.2018.29.4.527>
- Gracia-Palencia, A.J., Santini-Bell, E., Sipple, J.D. and Sanayi, M. (2015), "Structural model updating of an in-service bridge using dynamic data", *Struct. Control Health Monitor.*, **22**(10), 1265-1281. <https://doi.org/10.1002/stc.1742>
- Hou, Z., Xia, H., Y. W., Zhang, Y. and Zhang, T. (2015), "Dynamic analysis and model test on steel-concrete composite beams under moving loads", *Steel Compos. Struct., Int. J.*, **18**(3), 565-582. <https://doi.org/10.12989/scs.2015.18.3.565>
- Huo, R., Liu, W., Wu, P. and Zhou, D. (2017), "Analytical solutions for sandwich plates considering permeation effect by 3-D elasticity theory", *Steel Compos. Struct., Int. J.*, **25**(2), 127-139. <https://doi.org/10.12989/scs.2017.25.2.127>
- Kahya, V. and Turan, M. (2018), "Vibration and buckling of laminated beams by a multi-layer finite element model", *Steel Compos. Struct., Int. J.*, **28**(4), 415-426. <https://doi.org/10.12989/scs.2018.28.4.415>
- Karabelivo, K., Cue'llar, P., Baebler, M. and Rucker, W. (2015), "System identification of inverse, multimodal and nonlinear problem using evolutionary computing-application to a pile structure supported in nonlinear springs", *Eng. Struct.*, **101**, 609-620. <https://doi.org/10.1016/j.engstruct.2015.07.034>
- Khayat, M., Poorveis, D. and Moradi, S (2017), "Buckling analysis of functionally graded truncated conical shells under external displacement-dependent pressure", *Steel Compos. Struct., Int. J.*, **23**(1), 1-16. <https://doi.org/10.12989/scs.2017.23.1.001>
- Kumar, P. and Srinivas, J. (2018), "Transient vibration analysis of FG-MWCNT reinforced composite plate resting on foundation", *Steel Compos. Struct., Int. J.*, **29**(5), 569-578. <https://doi.org/10.12989/scs.2018.29.5.569>
- Lee, J.W., Coi, K.H. and Huh, Y.C. (2010), "Damage detection method for large structures using static and dynamic strain data from distributed fiber optic sensor", *Int. J. Steel Struct.*, **10**(1), 91-97. <https://doi.org/10.1007/BF03249515>
- Lei, J., Lozano-Galant, J.A., Nogal, M., Xu, D. and Turmo, J. (2016), "Analysis of measurement and simulation errors in structural system identification by observability techniques", *Struct. Control Health Monitor.*, **24**(6), e1923. <https://doi.org/10.1002/stc.1923>
- Lei, J., Xu, D. and Turmo, J. (2017a), "Static structural system identification for beam-like structures using compatibility conditions", *Struct. Control Health Monitor.*, **25**(1), e2062. <https://doi.org/10.1002/stc.2062>
- Lei, J., Nogal, M., Lozano-Galant, J.A., Xu, D. and Turmo, J. (2017b), "Constrained observability method in static structural system identification", *Struct. Control Health Monitor.*, **25**(1), e2040. <https://doi.org/10.1002/stc.1766>
- Lei, J., Lozano-Galant, J.A., Xu, D. and Turmo, J. (2019), "Structural system identification by measurement error-minimizing observability method", *Struct. Control Health Monitor.*, e2425. <https://doi.org/10.1002/stc.2425>
- Li, J., Huo, Q., Li, X., Kong, X. and Wu, W. (2014), "Dynamic stiffness analysis of steel-concrete composite beams", *Steel Compos. Struct., Int. J.*, **16**(6), 577-593. <https://doi.org/10.12989/scs.2014.16.6.577>
- Li, Z., Park, H.S. and Adeli, H. (2017a), "New method for modal identification of super high-rise building structures using discretized synchrosqueezed wavelet and Hilbert transforms", *Struct. Des. Tall Special Build.*, **26**(3), e1312. <https://doi.org/10.1002/tal.1312>
- Li, J., Jiang, L. and Li, X. (2017b), "Free vibration of a steel-concrete composite beam with coupled longitudinal and bending motions", *Steel Compos. Struct., Int. J.*, **24**(1), 79-91. <https://doi.org/10.12989/scs.2017.24.1.079>
- Liao, J., Tang, G., Meng, L., Liu, H. and Zhang, Y. (2012), "Finite element model updating based on field quasi-static generalized influence line and its bridge engineering application", *Procedia Eng.*, **31**, 348-353. <https://doi.org/10.1016/j.proeng.2012.01.1035>
- Lozano-Galant, J.A., Nogal, M., Castillo, E. and Turmo, J. (2013), "Application of observability techniques to structural system identification", *Comput.-Aided Civil Infrastruct. Eng.*, **28**(6), 434-450. <https://doi.org/10.1111/mice.12004>
- Lozano-Galant, J.A., Nogal, M., Paya-Zaforteza, I. and Turmo, J. (2014), "Structural system identification of cable-stayed bridges with observability techniques", *Struct. Infrastruct. Eng.*, **10**(11), 1331-1344. <https://doi.org/10.1080/15732479.2013.807292>
- Lozano-Galant, J.A., Nogal, M., Turmo, J. and Castillo, E. (2015), "Selection of measurement sets in static structural identification of bridges using observability trees", *Comput. Concrete, Int. J.*, **15**(5), 771-794. <https://doi.org/10.12989/cac.2015.15.5.771>
- MATLAB and Optimization Toolbox Release (2017), The MathWorks, Inc., Natick, MA, USA.
- Mei, L., Mita, A. and Zhou, J. (2016), "An improved substructural damage detection approach of shear structure based on ARMAX model residual", *Struct. Control Health Monitor.*, **23**(2), 218-236. <https://doi.org/10.1002/stc.1766>
- Nguyen, D.K. and Tran, T.T. (2018), "Free vibration of tapered BFGM beams using an efficient shear deformable finite element model", *Steel Compos. Struct., Int. J.*, **29**(3), 363-377. <https://doi.org/10.12989/scs.2018.29.3.363>
- Nogal, M., Lozano-Galant, J.A., Turmo, J. and Castillo, E. (2015), "Numerical damage identification of structures by observability techniques based on static loading tests", *Struct. Infrastruct. Eng.*, **12**(9), 1216-1227. <https://doi.org/10.1080/15732479.2015.1101143>
- Pajonk, O. (2009), "Overview of System Identification with Focus on Inverse Modeling", *Technische Universität Braunschweig*, 63.
- Pisano, A.A. (1999), "Structural System Identification: Advanced Approaches and Applications", PhD. Dissertation; Università di Pavia, Italy.
- Przemieniecki, J.S. (1968), *Theory of Matrix Structural Analysis*, Library of Congress Catalog Card Number.
- Sayyad, A.S. (2011), "Comparison of various refined beam theories for the bending and free vibration analysis of thick beams", *Appl. Computat. Mech.*, **5**, 217-230.
- Singh, S.K. and Chakrabarti, A. (2017), "Hygrothermal analysis of laminated composites using C0 FE model based on higher order zigzag theory", *Steel Compos. Struct., Int. J.*, **23**(1), 41-51. <https://doi.org/10.12989/scs.2017.23.1.041>

- Sirca Jr., G.F. and Adeli, H. (2012), "System identification in structural engineering", *Scientia Iranica*, **19**(6), 1355-1364.
<https://doi.org/10.1016/j.scient.2012.09.002>
- Soto, I.L. and Rojas, A.L. (2017), "Modeling for fixed-end moments of I-sections with straight haunches under concentrated load", *Steel Compos. Struct., Int. J.*, **23**(5), 597-610.
<https://doi.org/10.12989/scs.2017.23.5.597>
- Thirumalaiselvi, A., Anandavalli, N., Rajasankar, J. and Iyer, N.R. (2016), "Numerical evaluation of deformation capacity of laced steel-concrete composite beams under monotonic loading", *Steel Compos. Struct., Int. J.*, **20**(1), 167-184.
<https://doi.org/10.12989/scs.2016.20.1.167>
- Timoshenko, S.P. (1921), "On the correction for shear of the differential equation for transverse vibrations of prismatic bars", *Philosophical Magazine*, **41**(6), 744-746.
<https://doi.org/10.1080/14786442108636264>
- Tomas, D., Lozano-Galant, J.A., Ramos, G. and Turmo, J. (2018), "Structural system identification of thin web bridges by observability techniques considering shear deformation", *Thin-Wall. Struct.*, **123**, 282-293.
<https://doi.org/10.3390/s18040970>
- Vicente, M.A., Gonzalez, D.C., Minguez, J. and Schumacher, T. (2018), "A novel laser and video-based displacement transducer to monitor bridge deflections", *Sensors*, **18**(4), 970-985.
<https://doi.org/10.3390/s18040970>
- Walsh, B.J. and González, A. (2009), "Assessment of the condition of a beam using a static loading test", *Key Eng. Mater.*, **413-414**, 269-276.
<https://doi.org/10.4028/www.scientific.net/KEM.413-414.269>
- Wang, J., Li, T. and Luo, L. (2018), "Theoretical and experimental study on deflection of steel-concrete composite truss beams", *Steel Compos. Struct., Int. J.*, **29**(1), 91-106.
<https://doi.org/10.12989/scs.2018.29.1.091>
- Yan, A. and Golinval, J. (2005), "Structural damage localization by combining flexibility and stiffness methods", *Eng. Struct.*, **27**(12), 1752-1761.
<https://doi.org/10.1016/j.engstruct.2005.04.017>
- Yang, Y., Chen, Y., Zhang, J., Xue, Y., Liu, R. and Yu, Y. (2018), "Experimental investigation on shear capacity of partially prefabricated steel reinforced concrete columns", *Steel Compos. Struct., Int. J.*, **28**(1), 73-82.
<https://doi.org/10.12989/scs.2018.28.1.073>